REPORT DOCUMENTATION PAGE

Form Approved
OMB No. 0704-0188

1. REPORT DATE *(DD-MM-YYYY)*	**2. REPORT TYPE**	**3. DATES COVERED** *(From - To)*
20-09-2005	Conference Paper Preprint	2005

4. TITLE AND SUBTITLE
Sequential Multisine Excitation Signals for System Identification of Large Space Structures

5a. CONTRACT NUMBER

5b. GRANT NUMBER

5c. PROGRAM ELEMENT NUMBER

6. AUTHOR(S)
Jesse B. Hoagg, Seth L. Lacy,* Vit Babuska**

5d. PROJECT NUMBER
SAFF

5e. TASK NUMBER
SA

5f. WORK UNIT NUMBER
51

7. PERFORMING ORGANIZATION NAME(S) AND ADDRESS(ES) AND ADDRESS(ES)
Department of Aerospace Engrg
The University of Michigan
Ann Arbor, MI 48109

*Air Force Research Laboratory
Space Vehicles
3550 Aberdeen Ave SE
Kirtland AFB, NM 87117-5776

8. PERFORMING ORGANIZATION REPORT NUMBER

9. SPONSORING / MONITORING AGENCY NAME(S) AND ADDRESS(ES)
Air Force Research Laboratory
Space Vehicles
3550 Aberdeen Ave SE
Kirtland AFB, NM 87117-5776

10. SPONSOR/MONITOR'S ACRONYM(S)
AFRL/VSSV

11. SPONSOR/MONITOR'S REPORT NUMBER(S)

12. DISTRIBUTION / AVAILABILITY STATEMENT

Approved for public release; distribution is unlimited.

13. SUPPLEMENTARY NOTES Submitted to American Control Conference, Minneapolis, MN, 7 Oct 05.
Government Purpose Rights
**General Dynamics AIS

14. ABSTRACT
Linear system identification of complex nonlinear systems, such as large space structures, can be difficult because such systems are often lightly damped, have dense modal spacing, respond to disturbances over a large frequency bandwidth, and exhibit nonlinear responses. Many excitation signals used to collect frequency response data for linear system identification are poorly suited to systems that exhibit nonlinear responses. Specifically, random noise, burst random noise, pulse-impact, and multisine excitation signals can create undesired non-linear distortions in the frequency response data that are generally indistinguishable from the linear frequency response. Thus, sine dwell (also called stepped sine) excitation signals are often used to obtain frequency response to be separated from higher order harmonics. However, sine dwell testing can be very time consuming. In this paper, we present a novel sequence of multisine excitation signals that are more time efficient than sine dwell excitation while eliminating the effects of nonlinearity induced harmonics from the frequency response data. The sequential multisine excitation signal is demonstrated on the Deployable Optical Telescope testbed at Air Force Research Laboratory.

15. SUBJECT TERMS
Space Vehicles, Linear System Identification, Deployable Optical Telescope, Sequential Multisine Excitation Signal

16. SECURITY CLASSIFICATION OF:			**17. LIMITATION OF ABSTRACT**	**18. NUMBER OF PAGES**	**19a. NAME OF RESPONSIBLE PERSON**
a. REPORT	**b. ABSTRACT**	**c. THIS PAGE**			Seth L. Lacy
Unclassified	Unclassified	Unclassified	Unlimited	23	**19b. TELEPHONE NUMBER** *(include area code)* 505-853-3176

Standard Form 298 (Rev. 8-98)
Prescribed by ANSI Std. 239.18

Sequential Multisine Excitation Signals for System Identification of Large Space Structures

Jesse B. Hoagg
Department of Aerospace Engineering
The University of Michigan
Ann Arbor, MI 48109
jhoagg@umich.edu

Seth L. Lacy
Air Force Research Laboratory
Space Vehicles Directorate
Kirtland AFB, NM 87117
seth.lacy@kirtland.af.mil

Vit Babuška
General Dynamics AIS
vit.babuska@kirtland.af.mil

September 6, 2005

Abstract

Linear system identification of complex nonlinear systems, such as large space structures, can be difficult because such systems are often lightly damped, have dense modal spacing, respond to disturbances over a large frequency bandwidth, and exhibit nonlinear responses. Many excitation signals used to collect frequency response data for linear system identification are poorly suited to systems that exhibit nonlinear responses. Specifically, random noise, burst random noise, pulse-impact, and multisine excitation signals can create undesired nonlinear distortions in the frequency response data that are generally indistinguishable from the linear frequency response. Thus, sine dwell (also called stepped sine) excitation signals are often used to obtain frequency response data since sine dwell excitation signals allow the base tone response to be separated from higher order harmonics. However, sine dwell testing can be very time consuming. In this paper, we present a novel sequence of multisine excitation signals that are more time efficient than sine dwell excitation while eliminating the effects of nonlinearity induced harmonics from the frequency response data. The sequential multisine excitation signal is demonstrated on the Deployable Optical Telescope testbed at Air Force Research Laboratory.

1 Introduction

Large space structures often require vibration suppression to meet performance requirements. Strict performance requirements over large frequency bandwidths often prevent passive vibration isolation. Active control can be used to achieve high levels of disturbance rejection. However, many active control methods require high fidelity linear dynamic models that approximate the underlying dynamics. In addition, high fidelity models are required for performance prediction. Identifying linear dynamic models of large space structures can be difficult because large space structures are lightly damped, have dense modal spacing, have large dynamic range, respond to disturbances over a large frequency bandwidth, and may exhibit nonlinear responses.

There are numerous excitation signals used for linear system identification in the frequency domain, including random noise, burst random noise, pulse-impact, multisine, and sine dwell (also called stepped sine) [1–8]. Many excitation signals used to collect frequency response data are poorly suited to systems that exhibit nonlinear responses. Specifically, the nonlinear responses to these excitations creates undesired artifacts in the frequency response data. Furthermore, these undesired artifacts are indistinguishable from the linear frequency response and can significantly impact the characteristics of a linear model identified using frequency domain system identification methods.

In particular, it is difficult to use broadband excitation signals to obtain linear frequency response data for a system that exhibits nonlinear distortions due to harmonics. In [4, 5], it is suggested that a multisine excitation signal may be designed to reduced or eliminated nonlinear distortions. Specifically, nonlinear distortions may be eliminated by removing the appropriate harmonics from a multisine excitation signal. For example, if there is a nonlinearity that excites the odd harmonics of frequency f_1, then the odd harmonics of f_1 should be removed from the multisine excitation signal. However, this method requires certain knowledge of the system's nonlinearities, that is, we must know the harmonics that are being excited. In addition, the method suggested in [4, 5] is difficult to implement when the system has dense modal spacing and/or there are many base tones for which higher-order harmonics are being excited. Therefore, sine dwell excitation signals are often used to eliminate nonlinear distortions. However, sine dwell testing can be much less time efficient than broadband excitation signals [7]. In practice, sine dwell testing is often abbreviated, resulting in lower quality data.

In the present paper, we consider a novel sequence of multisine excitation signals designed to obtain system identification data over a large frequency bandwidth, while eliminating nonlinearity induced harmonics from the frequency response data. Furthermore, the method presented in this paper is more time efficient than sine dwell testing.

In Section 2, we formulate the excitation signal design problem. The properties of random noise, burst random noise, pulse-impact, multisine, and sine dwell excitation signals are reviewed in Sections 3-5. Section 6 compares the test times associated with multisine and sine dwell excitation signals. Sequential multisine excitation signals are presented in Section 7. Section 8 provides a sequential multisine implementation for multi-input systems. A simple numerical example is given in Section 9. In Section 10, experimental results are given

for the Deployable Optical Telescope (DOT) testbed at the Air Force Research Laboratory (AFRL). Conclusions are given in Section 11.

2 Problem Formulation

The goal of frequency domain system identification is to obtain a linear time-invariant model which approximates the dynamics of an unknown plant. In general, the plant may have nonlinear time-varying dynamics. Plant nonlinearities often induce harmonic responses to sinusoidal input signals. Consider, for example, the nonlinear system shown in Figure 1, which has asymptotically stable linear dynamics $\mathcal{L}$ with a static input nonlinearity $\mathcal{N}_1$ and a static output nonlinearity $\mathcal{N}_2$. The nonlinearities $\mathcal{N}_1$ and $\mathcal{N}_2$ of this system can induce harmonic responses. In particular, if $\mathcal{N}_1$ and $\mathcal{N}_2$ are analytic functions, then the nonlinearities can only induce integer superharmonics. If $\mathcal{N}_1$ and $\mathcal{N}_2$ are analytic functions, then they can be approximated to arbitrary accuracy by polynomials, that is,

$$\mathcal{N}_1(x) = \alpha_0 + \alpha_1 x + \cdots + \alpha_{n-1}x^{n-1} + \alpha_n x^n + \cdots , \tag{2.1}$$

$$\mathcal{N}_2(x) = \beta_0 + \beta_1 x + \cdots + \beta_{n-1}x^{n-1} + \beta_n x^n + \cdots , \tag{2.2}$$

where the real coefficients $\alpha_0, \alpha_1, \ldots$ and $\beta_0, \beta_1, \ldots$ are determined by the Taylor series expansions of $\mathcal{N}_1$ and $\mathcal{N}_2$, respectively. Now, we assume that the system input is the sinusoid

$$u(t) = C_1 \sin(2\pi\omega t) + C_2 \cos(2\pi\omega t\ ) . \tag{2.3}$$

Then the input to the linear dynamical system $\mathcal{L}$ is $u_{\mathcal{L}}(t) = \mathcal{N}_1(u(t))$. Using trigonometric identities, $u_{\mathcal{L}}(t)$ may be expressed as a sum of sinusoids with frequencies $\omega, 2\omega, 3\omega, \ldots$. Since $\mathcal{L}$ is an asymptotically stable linear system and $u_{\mathcal{L}}(t)$ is a sum of sinusoids with frequencies $\omega, 2\omega, 3\omega, \ldots$, it follows that the output $y_{\mathcal{L}}(t) = \mathcal{L}(\mathcal{N}_1(u(t)))$ at steady state is a sum of sinusoids with frequencies $\omega, 2\omega, 3\omega, \ldots$. Since $y_{\mathcal{L}}(t)$ is a sum of harmonically related sinusoids, we use the Taylor series expansion of $\mathcal{N}_2(x)$ and trigonometric identities to express $y(t) = \mathcal{N}_2(y_{\mathcal{L}}(t))$ as a sum of sinusoids with frequencies $\omega, 2\omega, 3\omega, \ldots$. Therefore, the nonlinearities $\mathcal{N}_1$ and $\mathcal{N}_2$ can induce integer superharmonic responses.

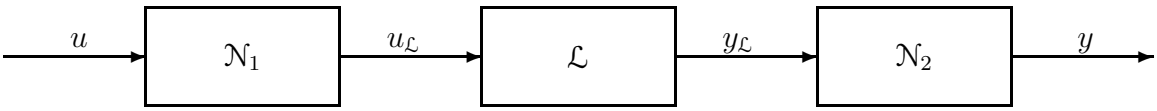

Figure 1: Linear dynamic system with static nonlinearities on the input and output.

In general, a system may have nonlinear time-varying dynamics that do not possess the block structure shown in Figure 1. In the present paper, we consider plants with nonlinear time-invariant dynamics and make the following assumptions.

(A1) The plant has a globally asymptotically stable equilibrium point.

(A2) The plant is linearizable about its globally asymptotically stable equilibrium.

(A3) The plant nonlinearities can induce only integer subharmonic and superharmonic responses of a base tone.

The objective of this paper is to design an excitation signal to obtain frequency response data for frequency domain system identification. We require that the excitation signal satisfies the following conditions.

(i) The signal must excite the frequency band $\Omega \triangleq [\omega_{\min}, \omega_{\max}]$, where $0 < \omega_{\min} < \omega_{\max}$.

(ii) The signal must be sufficiently rich to excite frequencies on a discrete grid with spacing less than or equal to η where $0 < \eta \leq \omega_{\min}$.

(iii) No leakage in the Fourier Transform of the excitation signal and output signal.

(iv) The base tone response of the plant must be distinguishable from nonlinear distortions caused by subharmonics and superharmonics.

Without loss of generality, we assume that $\frac{\omega_{\min}}{\eta}$ and $\frac{\omega_{\max}}{\eta}$ are integers.

In addition to conditions *(i)-(iv)*, we seek an input signal that does not require a long test time. Certain input signals can require long test times to meet conditions *(i)-(iv)*. In fact, test times can be too long for practical implementation. Thus, the purpose of this paper is to design an excitation signal that satisfies *(i)-(iv)*, while requiring test times short enough for practical implementation.

In the following sections, we examine the properties of several common excitation signals. Specifically, we consider random noise, burst random noise, pulse-impact, multisine, and sine dwell excitation signals. For more information on these input signals, see Chapter 4 of [8]. We demonstrate that none of these signals satisfies conditions *(i)-(iv)*, while being practically implementable with respect to test time.

In sections 3-7, we assume that the system is excited one input channel at a time. Thus, the test times derived in sections 3-7 are the required test times per input channel. More time efficient testing can be performed by simultaneously exciting all of the system's input channels. This case is discussed in Section 8.

3 Random Noise, Burst Random Noise, and Pulse-Impact

Random noise excitation requires a test time $T_{\mathrm{r}} \geq \frac{1}{\omega_{\min}}$ to achieve the desired frequency resolution and bandwidth. However, test times $T_{\mathrm{r}} >> \frac{1}{\omega_{\min}}$ are often required to infuse the frequency band Ω with sufficient power, to obtain a satisfactory signal-to-noise ratio, and to satisfy condition *(ii)*.

Random noise signals suffer from leakage since they are aperiodic. However, leakage can be alleviated by windowing the input and output data or by repeatedly applying an input signal [9]. Alternatively, leakage can be addressed by using burst random noise or pulse-impact excitation signals. Detailed discussions of burst random noise and pulse-impact

excitation signals are provided in [1, 2]. A burst random noise signal is

$$u_{\rm br}(t) = w(t)d(t), \tag{3.1}$$

where $w(t)$ is a random variable and $d(t) = \begin{cases} 1, & 0 \le t < T_1 \\ 0, & T_1 \le t \le T_{\rm r} \end{cases}$. A pulse-impact signal is

$$u_{\rm pi}(t) = \begin{cases} A_{\rm pi}, & 0 \le t < T_1 \\ 0, & T_1 \le t < T_{\rm r} \end{cases}, \tag{3.2}$$

where $A_{\rm pi} \in \mathbb{R}$. If the test time $T_{\rm r}$ is long enough so that the plant's response decays to a negligible amount by time $T_{\rm r}$, then leakage errors will be negligible [8]. However, for lightly damped systems with low frequency modes, the plant's response can take a long time to decay. In practice, windowing is often used with both burst random noise and pulse-impact excitation signals to allow for shorter test times.

To make matters worse, random and pulse excitation signals do not provide insight into the plant's nonlinearities. Specifically, the plant's linear response is indistinguishable from nonlinear distortions since random noise and pulse signals simultaneously excite the entire bandwidth of interest. Thus random noise, burst random noise, and pulse-impact signals do not satisfy condition *(iv)*.

4 Multisine

A multisine signal is a summation of sinusoids with varying frequencies and phases. A Schroeder-phased multisine is the sum of sinusoids where the phases are selected to obtain low peak-to-peak amplitudes [3]. Define $N \triangleq \frac{\omega_{\max}-\omega_{\min}}{\eta}+1$ and consider the Schroeder-phased multisine

$$u_{\rm m}(t) = \sum_{k=1}^{N} A_{\rm m} \cos\left(2\pi\omega_k t + \phi_k\right), \tag{4.1}$$

where $A_{\rm m} \in \mathbb{R}$ and, for $k = 1, \ldots, N$,

$$\phi_k \triangleq \frac{-k(k-1)\pi}{N}, \tag{4.2}$$

$$\omega_k \triangleq \omega_{\min} + \eta\left(k-1\right). \tag{4.3}$$

The Schroeder phases $\phi_1, \ldots, \phi_N$ have been used for simplicity. However, the phases may be selected to obtain other desired properties of the input signal. For example, the phases may be selected to minimize the crest-factor [10]. Note that the multisine (4.1) has a flat power spectrum over Ω.

The multisine is periodic with period $\frac{1}{\eta}$. Therefore, leakage is eliminated if

$$T_{\rm m} = l_{\rm m}\frac{1}{\eta} + \Delta t_{\rm m}, \tag{4.4}$$

where $l_{\mathrm{m}} \in \mathbb{N}$ is the number of periods used for averaging and $\Delta t_{\mathrm{m}} > 0$ is the time required for the system's response to $u_{\mathrm{m}}(t)$ to converge to steady state. Multisines can be efficient with respect to test time since they simultaneously excite the entire frequency band Ω and require only one settling period Δt_{m}.

However, simultaneous excitation of the entire bandwidth Ω is undesirable for dealing with nonlinearities. It is impossible to separate the linear response from harmonic responses caused by plant nonlinearities, and thus multisine excitation signals do not satisfy condition *(iv)*.

5 Sine Dwell

A sine dwell excitation signal is a sequence of sinusoidal excitation signals, each with different frequency. Define $N \stackrel{\triangle}{=} \frac{\omega_{\max}-\omega_{\min}}{\eta} + 1$ and, for $k = 1, \ldots, N$, consider the sinusoids

$$u_{\mathrm{s},k}(t) = A_{\mathrm{s},k} \sin\left(2\pi\omega_k t\right), \tag{5.1}$$

where for $k = 1, \ldots, N$, $A_{\mathrm{s},k} \in \mathbb{R}$ and $\omega_k \stackrel{\triangle}{=} \omega_{\min} + \eta\,(k-1)$. Sine dwell testing is performed by conducting the sequence of N sinusoidal inputs $u_{\mathrm{s},1}(t), \ldots, u_{\mathrm{s},N}(t)$. This populates the frequency band Ω with frequency spacing η.

The sinusoids $u_{\mathrm{s},1}(t), \ldots, u_{\mathrm{s},N}(t)$ are periodic with periods $\frac{1}{\omega_1}, \ldots, \frac{1}{\omega_N}$, respectively. For $k = 1, \ldots, N$, let $T_{\mathrm{s},k}$ be the measurement time associated with $u_{\mathrm{s},k}(t)$. Leakage is eliminated by letting $T_{\mathrm{s},k} = l_{\mathrm{s},k}\frac{1}{\omega_i}$ where, for $k = 1, \ldots, N$, $l_{\mathrm{s},k} \in \mathbb{N}$ is the number of periods used for averaging.

Unlike the other excitation signals we have discussed thus far, a sine dwell excitation signal allows the harmonic response to be separated from the base tone response. For $k = 1, \ldots, N$, the sinusoid $u_{\mathrm{s},k}(t)$ is used to estimate the base tone response at frequency ω_k, but the harmonic response can be distinguished from the base tone response since the harmonic responses due to nonlinearities occur at frequencies other than ω_k. In fact, sine dwell testing provides detailed information of nonlinear distortions.

However, the major drawback to sine dwell testing is lengthy test time. The test time required for sine dwell is

$$T_{\mathrm{s}} = \sum_{k=1}^{N} T_{\mathrm{s},k} + \Delta t_{\mathrm{s},k} = \sum_{k=1}^{N} l_{\mathrm{s},k}\frac{1}{\omega_k} + \Delta t_{\mathrm{s},k}, \tag{5.2}$$

where, for $k = 1, \ldots, N$, $\Delta t_{\mathrm{s},k} > 0$ is the time required for the system's response to the sinusoid $u_{\mathrm{s},k}(t)$ to settle. Sine dwell testing can require significantly longer test times than multisine testing.

Table 1 summarizes the properties of the excitation signals discussed in sections 3-5. Only sine dwell allows the linear frequency response to be separated from nonlinear distortions. However, sine dwell can require lengthy test times.

	Excites Ω	Frequency Spacing η	No Leakage	Removes Distortions due to Harmonics	Test Time T
Random Noise	✓	Often requires $T >> \frac{1}{\omega_{\min}}$	Requires windowing	No	Condition *(ii)* necessitates large T
Burst Random Noise	✓	Often requires $T >> \frac{1}{\omega_{\min}}$	Requires $T >> \frac{1}{\omega_{\min}}$ and/or windowing	No	Conditions *(ii)-(iii)* necessitates large T
Pulse-Impact	✓	Often requires $T >> \frac{1}{\omega_{\min}}$	Requires $T >> \frac{1}{\omega_{\min}}$ and/or windowing	No	Conditions *(ii)-(iii)* necessitates large T
Multisine	✓	✓	✓	No	More time efficient
Sine Dwell	✓	✓	✓	✓	Can require large T

Table 1: Properties of random noise, burst random noise, pulse-impact, multisine, and sine dwell excitation signals.

6 Test Times for Multisine and Sine Dwell Excitation

In this section, we compare the test times required for multisine and sine dwell excitation signals. Specifically, we compare the test times required to obtain frequency response data with equivalent signal-to-noise ratios. The quality of system identification data is most accurately described by the signal-to-noise ratios of the input and output signals. However, input signals are usually assumed to be noise-free, and the output signal-to-noise ratio depends on the output noise, the input power spectral density, and the system dynamics. If the system is linear, then the output power spectral density is the product of the input power spectral density and the magnitude of the system's transfer function. Although this paper considers nonlinear systems, if input amplitudes are small, then the output power spectral density is approximated by the product of input power spectral density and the magnitude of the linearized transfer function. We use the signal-to-noise ratio obtained from the approximate output power spectral density as a measure of data quality.

Let F_s denote the sampling frequency of the multisine and sine dwell excitation signals. The discrete Fourier transform of one period of the multisine $u_{\mathrm{m}}(t)$ is

$$U_{\mathrm{m}}(k) = \sqrt{\frac{F_s}{\eta}} \frac{A_{\mathrm{m}}}{2}, \tag{6.1}$$

and the discrete Fourier transform of an excitation signal consisting one period of each sine dwell $u_{\mathrm{s},1}(t), \ldots, u_{\mathrm{s},N}(t)$ is

$$U_{\mathrm{s}}(k) = \sqrt{\frac{F_s}{\omega_k}} \frac{A_{\mathrm{s},k}}{2}. \tag{6.2}$$

Assumption (A1) implies that the excitation signals are for linearizable systems, so let $G(z)$ be the discrete transfer function matrix of the linearized and sampled system. Then the approximate output power spectral densities obtained from multisine and sine dwell excitation are

$$Y_{\mathrm{m}}(k) \triangleq ||G(e^{\jmath\omega_k})||\, U_{\mathrm{m}}(k) = \sqrt{\frac{F_s}{\eta}} \frac{A_{\mathrm{m}}}{2} ||G(e^{\jmath\omega_k})||\,, \tag{6.3}$$

$$Y_{\mathrm{s}}(k) \triangleq ||G(e^{\jmath\omega_k})||\, U_{\mathrm{s}}(k) = \sqrt{\frac{F_s}{\omega_k}} \frac{A_{\mathrm{s},k}}{2} ||G(e^{\jmath\omega_k})||\,, \tag{6.4}$$

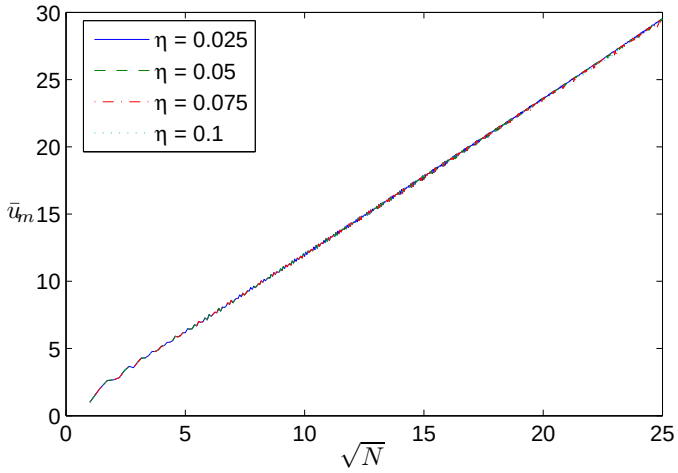

Figure 2: The peak signal value $\bar{u}_{\rm m}$ of a Schroeder-phase multisine versus $\sqrt{N}$. Various values of η are plotted where $\omega_{\rm min} = \eta$.

respectively.

Input amplitudes for the mutlisine and sine dwell excitation signals must be normalized to compare testing times, since linear approximations are only valid for small amplitudes and actuator saturation imposes practical limitations. If we design multisine and sine dwell excitation signals such that $A_{\rm m} = A_{{\rm s},1} = \cdots = A_{{\rm s},N} = A$ where $A > 0$, then the excitation signals will not have equal peak values. In fact, the peak value of a multisine increases with the number of sinusoids N, see Figure 2.

Define the peak value $\bar{u}_{\rm m} \triangleq \max_{0 \le t < \frac{1}{\eta}} \left| \sum_{k=1}^{N} \cos\left(2\pi\omega_k t + \phi_k\right) \right|$ of the Schroeder-phased multisine (4.1). Figure 2 provides plots of $\bar{u}_{\rm m}$ versus $\sqrt{N}$ for various values of η where $\omega_{\rm min} = \eta$. The numerical results indicate that the peak value of the Schroeder-phased multisine (4.1) is proportional to $\sqrt{N}$. Furthermore, the constant of proportionality is independent of the frequency spacing η.

Let $A_{{\rm s},1} = \cdots = A_{{\rm s},N} = A$ and $A_{\rm m} = \frac{A}{\sqrt{N}}$, where $A > 0$ is the desired peak signal value. We use the normalization $A_{\rm m} = \frac{A}{\sqrt{N}}$, which is convenient for the subsequent analysis, even though the constant of proportionality between $\bar{u}_{\rm m}$ and $\sqrt{N}$ is not exactly one. The approximate output power spectral densities satisfy

$$Y_{\rm m}(k) = \sqrt{\frac{F_s}{\eta}} \frac{A}{2\sqrt{N}} \left|\left| G(e^{\jmath\omega_k}) \right|\right|, \tag{6.5}$$

$$Y_{\rm s}(k) = \sqrt{\frac{F_s}{\omega_k}} \frac{A}{2} \left|\left| G(e^{\jmath\omega_k}) \right|\right|. \tag{6.6}$$

Let $N_y(k)$ denote the discrete Fourier transform of the output noise, then the output signal-to-noise ratio for a single period of the multisine excitation $u_{\rm m}(t)$ is

$$\frac{Y_{\rm m}(k)}{N_y(k)} = \frac{1}{\sqrt{\eta N}} \frac{A\sqrt{F_s}}{2N_y(k)} \left|\left| G(e^{\jmath\omega_k}) \right|\right|, \tag{6.7}$$

and the output signal-to-noise ratio for an excitation signal with a single period of each sine dwell $u_{\mathrm{s},1}(t), \ldots, u_{\mathrm{s},N}(t)$ is

$$\frac{Y_{\mathrm{s}}(k)}{N_y(k)} = \frac{1}{\sqrt{\omega_k}} \frac{A\sqrt{F_s}}{2N_y(k)} \left|\left|G(e^{\jmath\omega_k})\right|\right|. \tag{6.8}$$

The test times required for the multisine and sine dwell excitations are given by (4.4) and (5.2), respectively. However, the number of multisine periods l_{m} and sine dwell periods $l_{\mathrm{s},1}, \ldots, l_{\mathrm{s},N}$ used for averaging should be chosen to ensure that the output signals have comparable signal-to-noise ratios.

We assume that $N_y(k)$ is filtered white noise, independent of both $Y_{\mathrm{m}}(k)$ and $Y_{\mathrm{s}}(k)$, with a finite second moment. Under these mild assumptions averaging the output data over $l \in \mathbb{N}$ periods reduces the noise proportional to $\frac{1}{\sqrt{l}}$ [8]. Let $\mathrm{SNR}_{\mathrm{m}}(k)$ denote the output signal-to-noise ratio of the multisine excitation data when l_{m} averages are performed, and let $\mathrm{SNR}_{\mathrm{s}}(k)$ denote the output signal-to-noise ratio of the sine dwell excitation data when $l_{\mathrm{s},1}, \ldots, l_{\mathrm{s},N}$ averages are performed. Therefore, the signal-to-noise ratios satisfy

$$\mathrm{SNR}_{\mathrm{m}}(k) \propto \sqrt{l_{\mathrm{m}}} \frac{1}{\sqrt{\eta N}} \frac{A\sqrt{F_s}}{2N_y(k)} \left|\left|G(e^{\jmath\omega_k})\right|\right|, \tag{6.9}$$

and

$$\mathrm{SNR}_{\mathrm{s}}(k) \propto \sqrt{l_{\mathrm{s},k}} \frac{1}{\sqrt{\omega_k}} \frac{A\sqrt{F_s}}{2N_y(k)} \left|\left|G(e^{\jmath\omega_k})\right|\right|. \tag{6.10}$$

If $l_{\mathrm{s},k} = l\frac{\omega_k}{\eta}$ and $l_{\mathrm{m}} = lN$, then it follows from (6.9) and (6.10) that the output signals obtained from the multisine and sine dwell excitations have comparable signal-to-noise ratios. To obtain these comparable signal-to-noise levels, the multisine excitation signal requires

$$T_{\mathrm{m}} = l_{\mathrm{m}} \frac{1}{\eta} + \Delta t_{\mathrm{m}} = N \frac{l}{\eta} + \Delta t_{\mathrm{m}}, \tag{6.11}$$

and sine dwell excitation requires

$$T_{\mathrm{s}} = \sum_{k=1}^{N} l_{\mathrm{s},k} \frac{1}{\omega_k} + \Delta t_{\mathrm{s},k} = \sum_{k=1}^{N} \left(l \frac{\omega_k}{\eta} \right) \frac{1}{\omega_k} + \Delta t_{\mathrm{s},k} = N \frac{l}{\eta} + \sum_{k=1}^{N} \Delta t_{\mathrm{s},k}. \tag{6.12}$$

It follows from (6.11) and (6.12) that sine dwell testing can take significantly longer than multisine testing. Specifically, sine dwell testing requires additional time for the system to settle each time the sine dwell frequency is changed. For linear systems, practical settling times Δt_{m} and $\Delta t_{\mathrm{s},1}, \ldots, \Delta t_{\mathrm{s},N}$ can be estimated from the system's time constant. Furthermore, the time constant of a linear system is independent of input signal. Therefore, in practice, it is often assumed that settling time is independent of the harmonic content of the excitation signal.

If we assume that the settling times Δt_{m} and $\Delta t_{\mathrm{s},1}, \ldots, \Delta t_{\mathrm{s},N}$ are independent of excitation signal, then sine dwell testing requires $(N-1)\,\Delta t_{\mathrm{m}}$ time units longer than multisine

testing. If, in addition, the frequency band of interest is large and/or the frequency spacing is small, then N will be large and sine dwell testing will take significantly longer than multisine testing. Furthermore, if the system is lightly damped, then settling times can be very long, exacerbating the disparity in test times.

For example, consider a single-input system and design input signals to excite frequencies from $\omega_{\min} = 0.1$ Hz to $\omega_{\max} = 100$ Hz with a frequency spacing of $\eta = 0.1$ Hz. Assume that the system requires 5 seconds to settle. The multisine signal (4.1) requires

$$T_{\mathrm{m}} = N\frac{l}{\eta} + \Delta t_{\mathrm{m}} = 10,000l + 5 \text{ sec}, \tag{6.13}$$

and the sine dwell signal (5.1) requires

$$T_{\mathrm{s},k} = N\frac{l}{\eta} + \sum_{k=1}^{N} \Delta t_{\mathrm{s},k} = 10,000l + 5,000 \text{ sec}. \tag{6.14}$$

Thus, sine dwell testing requires an additional 4,995 seconds (or 1 hour 23 minutes 15 seconds). If l is small, then 4,995 seconds constitutes a significant portion of the total testing time. Furthermore, if the frequency band Ω is increased or the frequency spacing η is decreased, then the disparity between the sine dwell test time and the multisine test time will increase.

7 Sequential Multisines

In this section, we present a novel excitation signal consisting of a sequence of multisines that are designed to retain the benefits of sine dwell signals while being more time efficient. Specifically, we design a sequence of multisines that allow the linear response to be distinguished from nonlinear distortions.

Let $M \in \mathbb{N}$ be the least positive integer such that $M > \log_2 \frac{\omega_{\max}}{\omega_{\min}}$. In general, $M \leq N$ and if the bandwidth of interest is large and/or η is small, then $M << N$.

Now, we divide the frequency band Ω into M segments. For $i = 1, \ldots, M$, define the frequency bands

$$\Omega_i \triangleq [\bar{\omega}_i, \bar{\omega}_{i+1}), \tag{7.1}$$

where, for $i = 1, \ldots, M$,

$$\bar{\omega}_i \triangleq 2^{i-1}\omega_{\min}, \tag{7.2}$$

and $\bar{\omega}_{M+1} \triangleq \omega_{\max} + \eta$. Note that, for $i = 1, \ldots, M$, Ω_i does not contain integer subharmonics or superharmonics of the base frequencies contained in Ω_i.

Now, we consider a sequence of M Schroeder-phased multisines. For $i = 1, \ldots, M$, define $N_i \triangleq \frac{\bar{\omega}_{i+1} - \bar{\omega}_i}{\eta}$ and consider

$$u_{\mathrm{sm},i}(t) = \sum_{j=1}^{N_i} A_{\mathrm{sm},i} \cos\left(2\pi\omega_{i,j}t + \phi_{i,j}\right), \tag{7.3}$$

where, for $i = 1, \ldots, M$, $A_{\mathrm{sm},i} \in \mathbb{R}$ and, for $j = 1, \ldots, N_i$,

$$\phi_{i,j} \triangleq \frac{-j(j-1)\pi}{N_i}, \tag{7.4}$$

$$\omega_{i,j} \triangleq \bar{\omega}_i + \eta\,(j-1)\,. \tag{7.5}$$

If, for example, $\omega_{\min} = \eta$, then $N_1 = 1$, $N_2 = 2$, $N_3 = 4$, $N_4 = 8, \ldots, N_{M-1} = 2^{M-2}$ and $N_M = 2^{M-2} + \frac{\omega_{\max}}{\eta} + 1$. Again, the Schroeder phases have been chosen for simplicity, but the phases may be chosen to satisfy other excitation signal criteria.

For $i = 1, \ldots, M$, the multisine $u_{\mathrm{sm},i}(t)$ excites frequencies in the band Ω_i but does not excite frequencies outside of the band Ω_i. For $i = 1, \ldots, M$, let $T_{\mathrm{sm},i}$ be the measurement time associated with $u_{\mathrm{sm},i}(t)$. For $i = 1, \ldots, M$, letting $T_{\mathrm{sm},i} = l_{\mathrm{sm},i}\frac{1}{\eta}$ where $l_{\mathrm{sm},i} \in \mathbb{N}$ eliminates leakage. Then the test time required for the sequential multisine signal is given by

$$T_{\mathrm{sm}} = \sum_{i=1}^{M} T_{\mathrm{sm},i} + \Delta t_{\mathrm{sm},i} = \frac{1}{\eta}\sum_{i=1}^{M} l_{\mathrm{sm},i} + \Delta t_{\mathrm{sm},i}, \tag{7.6}$$

where, for $i = 1, \ldots, M$, $\Delta t_{\mathrm{sm},i} > 0$ is the time required for the system's response to $u_{\mathrm{sm},i}(t)$ to settle to harmonic steady state.

Now, we compare the sequential multisine test time with the multisine and sine dwell test times. For $i = 1, \ldots, M$, let $A_{\mathrm{sm},i} = \frac{A}{\sqrt{N_i}}$, thus normalizing the peak signal values to approximately $A > 0$. The number of sequential multisine periods $l_{\mathrm{sm},1}, \ldots, l_{\mathrm{sm},M}$ used for averaging must be chosen to ensure that the output signal obtained from the sequential multisine excitation has a signal-to-noise ratio comparable to those obtain from the multisine and sine dwell excitations.

For $i = 1, \ldots, M$, the discrete Fourier transform of a signal consisting of one period of each sequential multisine $u_{\mathrm{sm},1}, \ldots, u_{\mathrm{sm},M}$ is

$$U_{\mathrm{sm}}(k) = \sqrt{\frac{F_s}{\eta}}\frac{A}{2\sqrt{N_i}}, \quad \forall k \in [N_{i-1}, N_i]\,, \tag{7.7}$$

where $N_0 = 1$. Then, for $i = 1, \ldots, M$, the approximate output power spectral density is

$$Y_{\mathrm{sm}}(k) \triangleq \frac{1}{\sqrt{\eta N_i}}\frac{A\sqrt{F_s}}{2}\left|\left|G(e^{\jmath\omega_k})\right|\right|, \quad \forall k \in [N_{i-1}, N_i]\,, \tag{7.8}$$

which implies the output signal-to-noise ratio is

$$\frac{Y_{\mathrm{sm}}(k)}{N_y(k)} = \frac{1}{\sqrt{\eta N_i}}\frac{A\sqrt{F_s}}{2N_y(k)}\left|\left|G(e^{\jmath\omega_k})\right|\right|, \quad \forall k \in [N_{i-1}, N_i]\,. \tag{7.9}$$

Let $\mathrm{SNR}_{\mathrm{sm}}(k)$ denote the output signal-to-noise ratio of the sequential multisine excitation data when for $i = 1, \ldots, M$, $l_{\mathrm{sm},i}$ averages are performed. Then, for $i = 1, \ldots, M$,

$$\mathrm{SNR}_{\mathrm{sm}}(k) \propto \sqrt{l_{\mathrm{sm,i}}}\frac{1}{\sqrt{\eta N_i}}\frac{A\sqrt{F_s}}{2N_y(k)}\left|\left|G(e^{\jmath\omega_k})\right|\right|, \quad \forall k \in [N_{i-1}, N_i]\,. \tag{7.10}$$

If, for $i = 1, \ldots, M$, $l_{\mathrm{sm},i} = lN_i$, then $\mathrm{SNR}_{\mathrm{sm}}(k)$ is comparable to $\mathrm{SNR}_{\mathrm{m}}(k)$ and $\mathrm{SNR}_{\mathrm{s}}(k)$. To obtain this comparable signal-to-noise level, the sequential multisine excitation requires

$$T_{\mathrm{sm}} = \sum_{i=1}^{M} T_{\mathrm{sm},i} + \Delta t_{\mathrm{sm},i} = \frac{1}{\eta} \sum_{i=1}^{M} lN_i + \Delta t_{\mathrm{sm},i} = N\frac{l}{\eta} + \sum_{i=1}^{M} \Delta t_{\mathrm{sm},i}. \tag{7.11}$$

It follows from (6.11), (6.12), and (7.11) that sequential multisine testing is less time efficient than single multisine testing, but sequential multisine testing is more time efficient than sine dwell testing. In fact, if the system's settling times Δt_{m}, $\Delta t_{\mathrm{s},1}, \ldots, \Delta t_{\mathrm{s},N}$, and $\Delta t_{\mathrm{s},1}, \ldots, \Delta t_{\mathrm{s},N}$ are equal, then sine dwell testing takes $(N - M)\Delta t_{\mathrm{m}}$ more time units than sequential multisine testing. Furthermore, N increases quicker than M as the number of discrete frequency points increases. Specifically, N increases linearly with the number of discrete frequencies whereas M is proportional to the logarithm of the number of discrete frequencies. Therefore, $N - M$ may be very large.

Consider again the example given in Section 6. The objective is to design an input signal that excites frequencies from $\omega_{\min} = 0.1$ Hz to $\omega_{\max} = 100$ Hz with a discrete-frequency spacing of $\eta = 0.1$ Hz. We assume that for all harmonic excitations, the system requires 5 seconds to settle. Recall that the a single multisine requires a test time of $T_{\mathrm{m}} = 10,000l + 5$ sec, and a sine dwell input requires a test time of $T_{\mathrm{s}} = 10,000l + 5,000$ sec. In contrast, the sequential multisine (7.3) requires a test time

$$T_{\mathrm{sm}} = N\frac{l}{\eta} + \sum_{i=1}^{M} \Delta t_{\mathrm{sm},i} = 10,000l + 50 \text{ sec}. \tag{7.12}$$

Thus sine dwell excitation requires 4,950 seconds (or 1 hour 22 minutes 30 seconds) longer than sequential multisine excitation.

For $i = 1, \ldots, M$, $u_{\mathrm{sm},i}(t)$ is used to estimate the base tone response over the frequency band Ω_i, but the harmonic response due to nonlinearities occur at frequencies not contained in the Ω_i. Thus, the linear response over Ω_i is distinguishable from the nonlinear distortions that occur at frequencies outside of Ω_i. Thus, the sequential multisine satisfies conditions *(i)-(iv)* while being less time consuming than sine dwell testing.

8 Sequential Multisine Excitation for Multi-Input Systems

In the previous sections, we designed multisine, sine dwell, and sequential multisine excitation signals assuming that the system is excited one input at a time, that is, data is first taken by exciting input channel 1, then by exciting input channel 2, and continuing until the system has been excited through all input channels. Now, we assume that the system has p inputs. Then the test times given by (6.11), (6.12), and (7.11) are multiplied by p to yield the total test time.

For a sine dwell excitation signal, it is clear that exciting the system using only one input channel at a time is not time efficient. In fact, sine dwell testing can be performed by simultaneously exciting all input channels. To ensure that we can distinguish between

the different input-to-output frequency responses, we require that no two input channels are simultaneously excited at the same frequency. Similarly, to ensure that the base tone response is distinguishable from the nonlinear distortions, we require that no two input channels be simultaneously excited at any harmonic of the same base frequency. Additionally, data must be taken for an integer number of periods at each frequency to avoid leakage in the Fourier Transform. Following these rules, the test time for sine dwell excitation is independent of the number of inputs.

Similarly, sequential multisine excitation signals can be designed so that all input channels may be excited simultaneously, yielding a test time that is independent of p. We consider the frequency bands $\Omega_1, \ldots, \Omega_M$ given by (7.3), and defined the finer frequency spacing $\bar{\eta} \triangleq \frac{\eta}{p}$. For each input channel, we consider a sequence of M Schroeder-phased multisines. For $i = 1, \ldots, M$, consider

$$u^1_{\mathrm{sm},i}(t) = \sum_{j=1}^{N_i} A_{\mathrm{sm},i} \cos\left(2\pi\left(\omega_{i,j}\right) t + \phi_{i,j}\right), \tag{8.1}$$

$$u^2_{\mathrm{sm},i}(t) = \sum_{j=1}^{N_i} A_{\mathrm{sm},i} \cos\left(2\pi\left(\omega_{i,j} + \bar{\eta}\right) t + \phi_{i,j}\right), \tag{8.2}$$

$$u^3_{\mathrm{sm},i}(t) = \sum_{j=1}^{N_i} A_{\mathrm{sm},i} \cos\left(2\pi\left(\omega_{i,j} + 2\bar{\eta}\right) t + \phi_{i,j}\right), \tag{8.3}$$

$$\vdots \tag{8.4}$$

$$u^p_{\mathrm{sm},i}(t) = \sum_{j=1}^{N_i} A_{\mathrm{sm},i} \cos\left(2\pi\left(\omega_{i,j} + (p-1)\,\bar{\eta}\right) t + \phi_{i,j}\right). \tag{8.5}$$

In this notation, input channel 1 is excited with the sequence of multisines $u^1_{\mathrm{sm},1}(t), \ldots, u^1_{\mathrm{sm},M}(t)$, input channel 2 is excited with the sequence of multisines $u^2_{\mathrm{sm},1}(t), \ldots, u^2_{\mathrm{sm},M}(t)$, and input channel p is excited with the sequence of multisines $u^p_{\mathrm{sm},1}(t), \ldots, u^p_{\mathrm{sm},M}(t)$.

For $i = 1, \ldots, M$, the multisines $u^1_{\mathrm{sm},i}(t), \ldots, u^p_{\mathrm{sm},i}(t)$ are periodic with period $\frac{1}{\bar{\eta}}$. Therefore, leakage is eliminated by letting the test time associated with each multisine in the sequence be $\bar{T}_{\mathrm{sm},i} = \bar{l}_{\mathrm{sm},i}\frac{1}{\bar{\eta}}$ where $\bar{l}_{\mathrm{sm},i} \in \mathbb{N}$. Since all input channels are simultaneously excited, the required test time is given by

$$T_{\mathrm{sm}} = \frac{1}{\bar{\eta}} \sum_{i=1}^{M} \bar{l}_{\mathrm{sm},i} + \bar{\Delta} t_{\mathrm{sm},i}, \tag{8.6}$$

where, for $i = 1, \ldots, M$, $\bar{\Delta} t_{\mathrm{sm},i}$ is the time required for the system's response to $u^1_{\mathrm{sm},i}(t), \ldots, u^p_{\mathrm{sm},i}(t)$ to settle.

If data is collected for at least $\frac{1}{\bar{\eta}}$ seconds and the settling time is independent of the excitation signal, then the test time required for sequential mutlisine excitation does not depend on the number of inputs. That is, the system can be excited though all channels simultaneously.

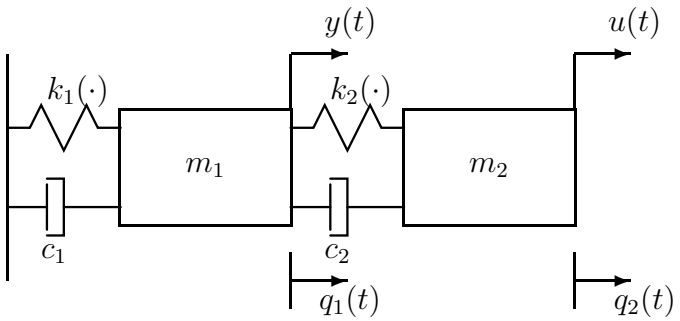

Figure 3: Two-degree-of-freedom spring-mass-damper with nonlinear stiffness.

9 Two-Degree-Of-Freedom Spring-Mass-Damper with Cubic Stiffness

Consider the two-degree-of-freedom spring-mass-damper with nonlinear stiffness shown in Figure 3. The dynamics of the system are

$$M\ddot{q} + C\dot{q} + K(q) = bu, \tag{9.1}$$

where

$$M \triangleq \begin{bmatrix} m_1 & \\ & m_2 \end{bmatrix}, \quad b \triangleq \begin{bmatrix} 0 \\ 1 \end{bmatrix}, \tag{9.2}$$

$$C \triangleq \begin{bmatrix} c_1 + c_2 & -c_2 \\ -c_2 & c_2 \end{bmatrix}, \tag{9.3}$$

$$K(q) \triangleq \begin{bmatrix} k_1(q_1) - k_2(q_2 - q_1) \\ k_2(q_2 - q_1) \end{bmatrix}, \tag{9.4}$$

$$q \triangleq \begin{bmatrix} q_1 & q_2 \end{bmatrix}^{\mathrm{T}}. \tag{9.5}$$

Assume that the nonlinear stiffness $k_1(\cdot)$ and $k_2(\cdot)$ are given by the cubic stiffness terms $k_1(x) \triangleq \tilde{k}_1 x + \hat{k}_1 x^3$ and $k_2(x) \triangleq \tilde{k}_2 x + \hat{k}_2 x^3$. The masses are $m_1 = m_2 = 0.1$ kg. The damping coefficients are $c_1 = 0.1$ kg/sec and $c_1 = 0.05$ kg/sec. The spring constants are $\tilde{k}_1 = 56$ kg/sec^2, $\tilde{k}_2 = 90$ kg/sec^2, and $\hat{k}_1 = \hat{k}_2 = 50$ kg/sec^2/m^2. The system (9.1)-(9.5) is linearizable about the origin, which is an asymptotically stable equilibrium. Let the output y be the position of the first mass, that is $y = q_1$. The linearized system from input u to output y is

$$u = G(s)y, \tag{9.6}$$

where

$$\begin{aligned} G(s) &\triangleq \frac{5s + 9000}{s^4 + 2s^3 + 2360.5s^2 + 1180s + 504000} \\ &= \frac{5s + 9000}{(s^2 + 0.374s + 237.464)(s^2 + 1.626s + 2122.4)}. \end{aligned} \tag{9.7}$$

The system has modes at approximately 2.45 Hz and 7.33 Hz. Now let us consider excitation signals designed for frequency domain system identification over the frequency band $\omega_{\min} = 0.1$ Hz and $\omega_{\max} = 25$ Hz with a frequency spacing of $\eta = 0.1$ Hz. The peak value of the excitation signal must be normalized to approximately $A = 0.25$.

We consider the following three excitation signals.

(1) The single multisine given by (4.1) where $N = 250$ and $A_{\rm m} = \frac{A}{\sqrt{N}} = \frac{0.25}{\sqrt{250}}$ N.

(2) The sine dwell signal (5.1) where $N = 250$ and $A_{{\rm s},1}, \ldots, A_{{\rm s},N} = 0.25$ N.

(3) The sequential multisine (7.3) where $M = 8 > \log_2(\frac{\omega_{\max}}{\omega_{\min}})$ and, for $i = 1, \ldots, M$, $A_{{\rm sm},i} = \frac{A}{\sqrt{N_i}}$ where $N_i = \frac{\bar{\omega}_{i+1} - \bar{\omega}_i}{\eta}$. Therefore, $A_{{\rm sm},1} = 0.25$ N, $A_{{\rm sm},2} \approx 0.1768$ N, $A_{{\rm sm},3} = 0.125$ N, $A_{{\rm sm},4} \approx 0.0884$ N, $A_{{\rm sm},5} = 0.0625$ N, $A_{{\rm sm},6} \approx 0.0442$ N, $A_{{\rm sm},7} \approx 0.0313$ N, and $A_{{\rm sm},8} \approx 0.0221$ N.

To obtain equivalent signal-to-noise ratios, the single multisine excitation is averaged over $l_{\rm m} = N$ periods, for $k = 1, \ldots, N$, the sine dwell excitations are averaged over $l_{{\rm s},k} = \frac{\omega_k}{\eta}$ periods, and, for $i = 1, \ldots, M$, the sequential multisine excitations are averaged over $l_{{\rm sm},i} = N_i$ periods.

To illustrate the effects of nonlinearity induced harmonics, we consider the case where there is no noise on the input or the output. We excite the system (9.1)-(9.5) using the single multisine excitation. The system is allowed $\Delta t_{\rm m} = 10$ sec to settle. Then data is collected for $l_{\rm m} = N = 250$ periods of the single multisine, yielding

$$T_{\rm m} = l_{\rm m} \frac{1}{\eta} + \Delta t_{\rm m} = 2,510 \text{ sec} = 41 \text{ min } 50 \text{ sec}. \tag{9.8}$$

The transfer function (9.7) of the linearized system and the frequency response data obtain using the single multisine are shown in Figure 4. Input-output data is collected for 2,500 sec at a sample rate of 500 Hz. To obtain the frequency response data, we use Welch's averaged periodogram method, averaging 250 square windows of 5,000 data points to obtain 5,000 fast Fourier transform points.

Next, we excite the system (9.1)-(9.5) with the sine dwell signal. The system is allowed $\Delta t_{{\rm s},1}, \ldots, \Delta t_{{\rm s},N} = 10$ sec to settle at each frequency. For $k = 1, \ldots, N$, we collect data for $l_{{\rm s},k} = \frac{\omega_k}{\eta} = k$ periods of the sinusoid $u_{{\rm s},k}(t)$. Thus,

$$T_{\rm s} = \sum_{k=1}^{N} l_{{\rm s},k} \frac{1}{\omega_k} + \Delta t_{{\rm s},k} = 5,000 \text{ sec} = 1 \text{ hr } 23 \text{ min } 20 \text{ sec}. \tag{9.9}$$

The transfer function (9.7) of the linearized system and the frequency response data obtain using the sine dwell input are shown in Figure 5.

Finally, the system (9.1)-(9.5) is excited with the sequential multisine, and allowed $\Delta t_{{\rm ms},1}, \ldots, \Delta t_{{\rm ms},M} = 10$ sec to settle. For $i = 1, \ldots, M$, we collect data for $l_{{\rm sm},i} = N_i$ periods of $u_{{\rm sm},i}(t)$, yielding

$$T_{\rm sm} = \sum_{i=1}^{M} l_{{\rm sm},i} \frac{1}{\eta} + \Delta t_{{\rm sm},i} = 2,580 \text{ sec} = 43 \text{ min}. \tag{9.10}$$

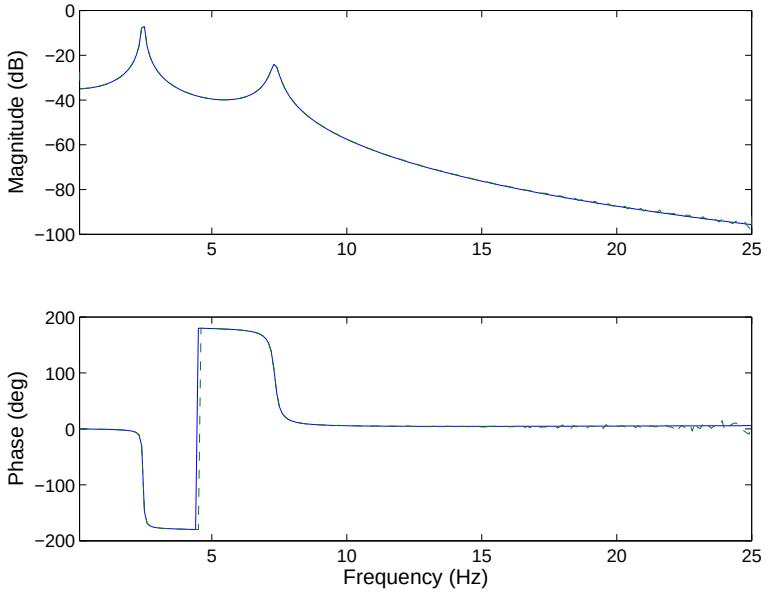

Figure 4: The transfer function of the linearized system (solid) and the frequency response data obtain using the single multisine excitation (dashed).

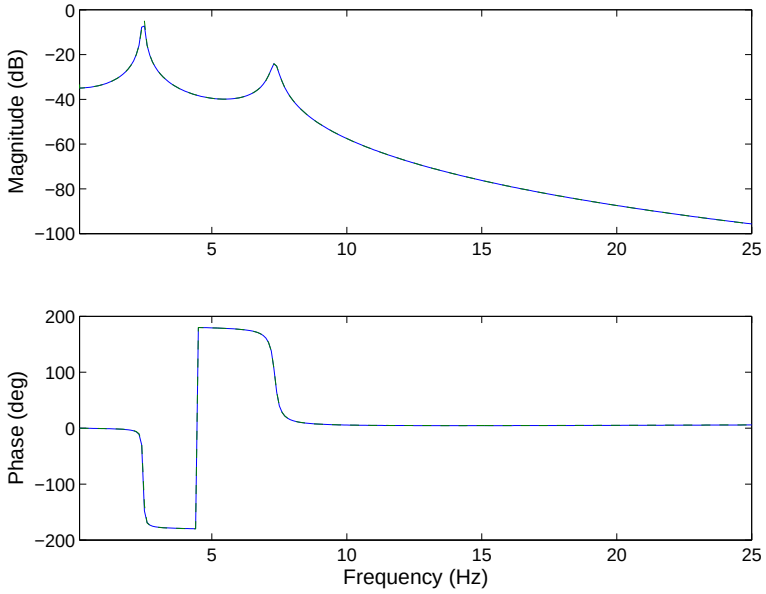

Figure 5: The transfer function of the linearized system (solid) and the frequency response data obtain using the sine dwell excitation (dashed).

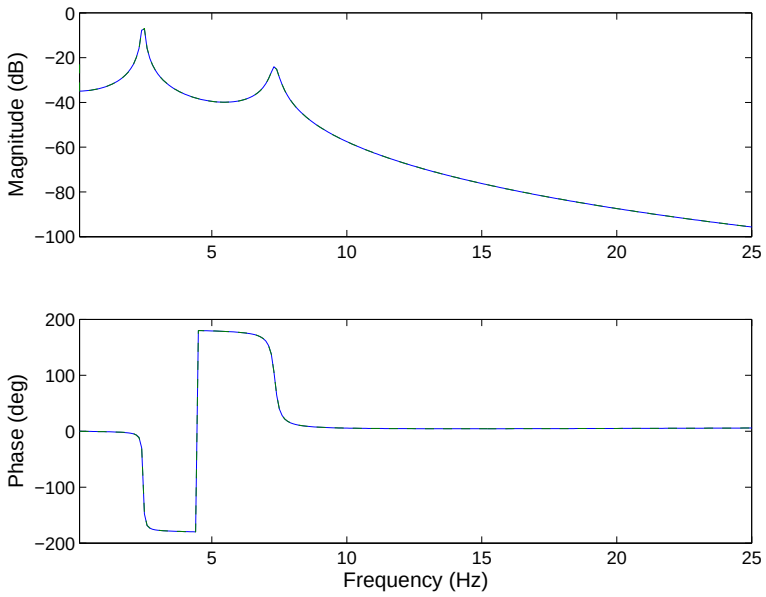

Figure 6: The transfer function of the linearized system (solid) and the frequency response data obtain using the sequential multisine excitation (dashed).

The transfer function (9.7) of the linearized system and the frequency response data obtain using the sequential multisine are shown in Figure 6.

Figures 4-6 illustrate that the frequency response data obtained from the single multisine excitation provides the poorest approximation the linearized dynamics. Nonlinear distortions in the frequency response occur above the 7.33 Hz mode and are a result of the third harmonic of the 2.45 Hz mode. The frequency response data obtained from the sine dwell excitation, shown in Figure 5, and the frequency response data obtained from the sequential multisine excitation, shown in Figure 6, both provide good approximations of the linearized dynamics. Furthermore, if the input and output data obtained from the sine dwell and sequential multisine excitations were corrupted by the same noise sequence, then the associated noise levels of the two sets of frequency response data would be comparable. However, the sine dwell testing takes 40 minutes 20 seconds longer than the sequential multisine testing.

10 Deployable Optical Telescope

The Deployable Optical Telescope (DOT) is a space-traceable sparse-aperture telescope developed by the Air Force Research Laboratory, see Figure 7. The weight and volume restrictions imposed by launch vehicles are the main impediments to fielding large aperture space telescopes. To alleviate volume restrictions, DOT's primary mirror segments and secondary mirror tower are deployable. Specifically, the primary mirror segments rotate into place via hinges and lock with latches. The secondary mirror tower slides into place and locks with latches.

A precise alignment of DOT's optical path is required to meet imaging requirements. Therefore, DOT requires active feedback control to reject image path disturbances caused

Figure 7: The Deployable Optical Telescope (DOT) testbed.

by, for example, thermal variations and the motion of the spacecraft's reaction wheels. Each primary mirror segment is actuated with three degrees of freedom, namely tip, tilt, and piston. The secondary tower is controlled using a piezo patch bonded to the tower. DOT uses laser metrology to provide optical-precision measurements for feedback control. Specifically, the laser metrology system provides tip, tilt, and piston measurements for each of the three primary mirror segments. In sum, DOT has 10 control inputs and 9 feedback measurements. For more information on DOT see [11–13].

High-fidelity linear dynamic models of DOT are required to design active feedback controllers that reject disturbances to DOT's optical path. However, obtaining input-output data for system identification of DOT is difficult because system nonlinearities induce harmonic responses [14]. Sine dwell excitation signals could be used to obtain frequency response data of DOT's base tone responses, but this would be very time consuming because performance objectives require frequency response data over a large frequency bandwidth (0 to 1000 Hz), and DOT has densely spaced modes, requiring frequency response data with a small frequency spacing. Therefore, system identification data may be obtained using the sequential multisine excitation signal.

Now, we compare the frequency response data obtained from DOT when using single multisine, sine dwell, and sequential multisine excitation signals. DOT is excited through the first actuator on the first primary mirror segment and the piston position of the first primary mirror segment is measured. Thus, we obtain frequency response data from the first actuator of the first mirror to the piston position of the first mirror. To compare the exictation signals, frequency response data is obtained over the frequency band $\omega_{\min} = 0.5$

Hz and $\omega_{\max} = 90$ Hz with a frequency spacing of $\eta = 0.5$ Hz. The peak value of the excitation signal must be normalized to approximately $A = 0.02$. We consider the following three excitation signals.

(1) The single multisine given by (4.1) where $N = 250$ and $A_{\mathrm{m}} = \frac{A}{\sqrt{N}} = \frac{0.02}{\sqrt{180}}$ N.

(2) The sine dwell signal (5.1) where $N = 180$ and $A_{\mathrm{s},1}, \ldots, A_{\mathrm{s},N} = 0.02$ N.

(3) The sequential multisine (7.3) where $M = 8 > \log_2(\frac{\omega_{\max}}{\omega_{\min}})$ and, for $i = 1, \ldots, M$, $A_{\mathrm{sm},i} = \frac{A}{\sqrt{N_i}}$ where $N_i = \frac{\bar{\omega}_{i+1} - \bar{\omega}_i}{\eta}$.

To obtain equivalent signal-to-noise ratios, the single multisine excitation is averaged over $l_{\mathrm{m}} = 360$ periods, for $k = 1, \ldots, N$, the sine dwell excitations are averaged over $l_{\mathrm{s},k} = 2\frac{\omega_k}{\eta}$ periods, and, for $i = 1, \ldots, M$, the sequential multisine excitations are averaged over $l_{\mathrm{sm},i} = 2N_i$ periods.

For all excitation signals, the system is allowed $\Delta t_{\mathrm{m}} = \Delta t_{\mathrm{s},1}, \ldots, \Delta t_{\mathrm{s},N} = \Delta t_{\mathrm{ms},1}, \ldots, \Delta t_{\mathrm{ms},M} = 10$ sec to settle. Therefore, the single multisine, sine dwell, and sequential multisine test times are

$$T_{\mathrm{m}} = l_{\mathrm{m}} \frac{1}{\eta} + \Delta t_{\mathrm{m}} = 730 \text{ sec} = 12 \text{ min } 10 \text{ sec}, \tag{10.1}$$

$$T_{\mathrm{s}} = \sum_{k=1}^{N} l_{\mathrm{s},k} \frac{1}{\omega_k} + \Delta t_{\mathrm{s},k} = 2,520 \text{ sec} = 42 \text{ min}, \tag{10.2}$$

$$T_{\mathrm{sm}} = \sum_{i=1}^{M} l_{\mathrm{sm},i} \frac{1}{\eta} + \Delta t_{\mathrm{sm},i} = 800 \text{ sec} = 13 \text{ min } 20 \text{ sec}, \tag{10.3}$$

respectively. Thus sine dwell testing takes significantly longer than single multisine or sequential multisine testing. However, single multisine testing cannot be used because of the harmonic distortion that results from system nonlinearities.

The data obtained from sine dwell excitation is used to calculate the total harmonic distortion of DOT's dynamics from the first actuator of the first mirror to the piston position of the first mirror. The total harmonic distortion is the ratio of output power at all superharmonic frequencies to the output power at the base frequency. Figure 8 shows that total harmonic distortion of DOT's dynamics from the first actuator of the first mirror to the piston position of the first mirror. Figure 8 demonstrates that there is significant harmonic distortion up to 10 Hz and lower levels of distortion at higher frequencies.

Figure 9 and 10 show the magnitude and the phase of the frequency response data obtained from the single multisine and sequential multisine excitation signals. The two frequency response differ most significantly between 0.5 and 30 Hz. This difference can be attributed to the harmonic distortion that is present in the single multisine data but is not present in the sequential multisine data.

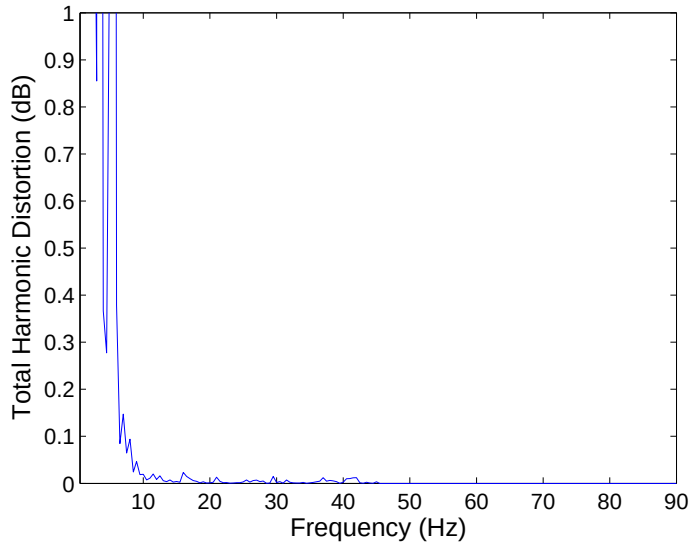

Figure 8: Total harmonic distortion from the control on the first primary mirror segment to the piston response of the first primary mirror segment.

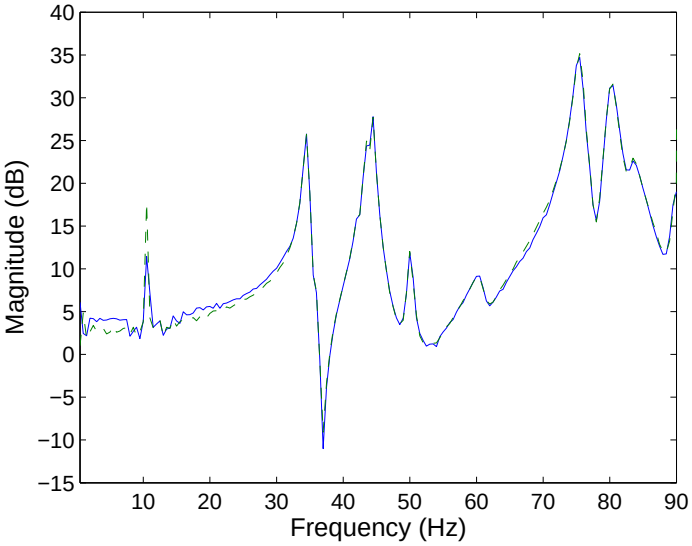

Figure 9: The magnitude of the frequency response data obtain using the sequential multisine excitation (solid) and the single multisine excitation (dashed).

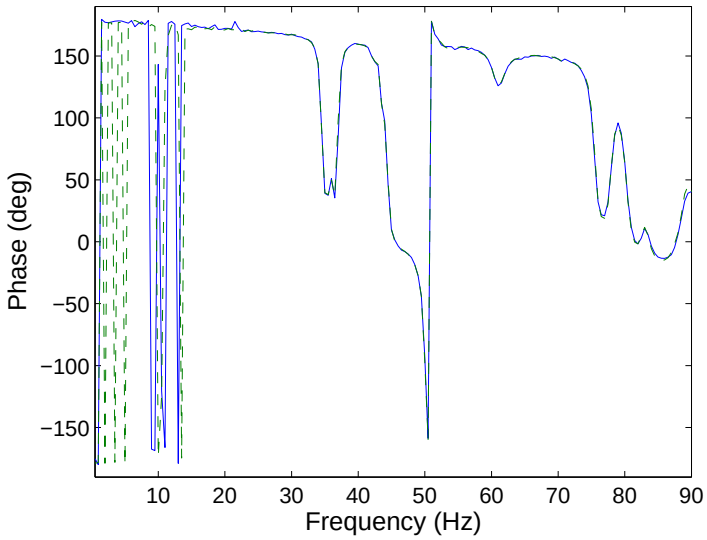

Figure 10: The phase of the frequency response data obtain using the sequential multisine excitation (solid) and the single multisine excitation (dashed).

11 Conclusions

Many excitation signals used to collect frequency response data for linear system identification are poorly suited to systems that exhibit nonlinear responses. Specifically, broadband excitation signals can create undesired nonlinear distortions in the frequency response data that are generally indistinguishable from the linear frequency response. Sine dwell excitation signals allow the base tone response to be separated from higher order harmonics. However, sine dwell testing can be very time consuming. In this paper, we presented a novel sequence of multisine excitation signals that are more time efficient than sine dwell excitation while eliminating the effects of nonlinearity induced harmonics from the frequency response data.

References

[1] N. Olsen, "Burst random excitation," *Sound and Vibration*, vol. 17, pp. 20–23, 1983.

[2] W. G. Halvorsen and D. L. Brown, "Impluse techniques for structural frequency response testing," *Sound and Vibration*, vol. 11, pp. 8–10,12–16,18–21, 1977.

[3] M. A. Schroeder, "Synthesis of low peak-factor signals and binary sequences of low autocorrelation," *IEEE Trans. Info. Theory*, vol. 16, pp. 85–89, 1970.

[4] M. W. Braun, R. Ortiz-Mojica, and D. E. Rivera, "Application of minimum crest factor multisinusoidal signals for "plant-friendly" identification of nonlinear process systems," *Contr. Eng. Practice*, vol. 10, pp. 301–313, 2002.

[5] H. A. Barker and K. R. Godfrey, "System identification with multi-level periodic perturbation signals," *Contr. Eng. Practice*, vol. 7, pp. 717–726, 1999.

[6] K. R. Godfrey, H. A. Barker, and A. J. Tucker, "Comparison of perturbation signals for linear system identification in the frequency domain," *IEE Prod. Contr. Thoery Appl.*, vol. 146, pp. 535–548, 1999.

[7] J. Schoukens, R. M. Pintelon, and Y. J. Rolain, "Broadband versus stepped sine frf measurements," *IEEE Trans. Instr. and Meas.*, vol. 49, pp. 275–278, 2000.

[8] R. Pintelon and J. Schoukens, *System Identification: A Frequency Domain Approach*. Piscataway, NJ: IEEE Press, 2001.

[9] I. I. Hussein, S. L. Lacy, and D. S. Bernstein, "Data compression for subspace-based identification using periodic inputs," in *Proc. Amer. Contr. Conf.*, May 2002, pp. 3313–3318.

[10] P. Guillaume, J. Schoukens, R. Pintelon, and I. Kollár, "Crest-factor minimization using nonlinear chebyshev approximation methods," *IEEE Trans. Instr. and Meas.*, vol. 40, pp. 982–989, 1991.

[11] K. D. Bell, R. L. Moser, M. K. Powers, and R. S. Erwin, "Deployable optical telescope ground demonstration," in *Proc. SPIE Vol. 4013: UV, Optical, and IR Space Telescopes and Instruments*, Munich, Germany, July 2000, pp. 559–567.

[12] K. N. Schrader, R. H. Fetner, J. Donaldson, R. J. Fuentes, and R. S. Erwin, "Integrated control system development for phasing and vibration suppression for a sparse-array telescope," in *Proc. SPIE Vol. 4849: Highly Innovative Space Telescope Concepts*, Waikoloa, HI, Dec 2002, pp. 134–145.

[13] K. N. Schrader, R. H. Fetner, S. F. Griffin, and R. S. Erwin, "Development of a sparse-aperture testbed for optomechanical control of space-deployable structures," in *Proc. SPIE Vol. 4849: Highly Innovative Space Telescope Concepts*, Waikoloa, HI, Dec 2002, pp. 384–395.

[14] S. L. Lacy, V. Babuška, K. N. Schrader, and R. Fuentes, "System identification of space structures," in *Proc. Amer. Contr. Conf.*, Portland, OR, June 2005, pp. 2335–2340.